EUV Multilayers for Solar Physics

D. L. Windt[1], S. Donguy[1], J. Seely[2], B. Kjornrattanawanich[3], E. M. Gullikson[4], C. C. Walton[5], L. Golub[6], and E. DeLuca[6]

[1]*Columbia University, 550 West 120th St, New York, NY 10027*
[2] *Naval Research Laboratory, 4555 Overlook Ave. S.W., Washington, DC 20375*
[3] *Universities Space Research Association, National Synchrotron Light Source, Beamline X24C, Brookhaven National Laboratory, Upton NY 11973*
[4]*Center For X-Ray Optics, Lawrence Berkeley National Laboratory, Berkeley, CA 94720*
[5]*Lawrence Livermore National Laboratory, Livermore, CA 94550*
[6]*Smithsonian Astrophysical Observatory, 60 Garden St, Cambridge, MA 02138*

ABSTRACT

We present an overview of currently available EUV multilayer coatings that can be used for the construction of solar physics instrumentation utilizing normal-incidence optics. We describe the performance of a variety of Si-based multilayers, including Si/B_4C and new Si/SiC films that provide improved performance in the wavelength range from 25 ñ 35 nm, as well as traditional Si/Mo multilayers, including broad-band coatings recently developed for the Solar-B/EIS instrument. We also outline prospects for operation at both longer and shorter EUV wavelengths, and also the potential of ultra-short-period multilayers that work near normal incidence in the soft X-ray region.

1. INTRODUCTION

The development in recent years of multilayer structures having nanometer-scale periods, designed as efficient reflective coatings in the extreme ultraviolet (EUV), has enabled the construction of new instrumentation utilizing normal-incidence multilayer optics for solar physics. High-resolution imagers comprising normal-incidence telescope mirrors coated with narrow-band multilayers tuned to specific coronal or transition-region emission lines have been used in a variety of missions, most notably the SOHO/EIT and TRACE satellite instruments; normal-incidence multilayer imagers will be used in future satellite missions as well, including STEREO, SDO, Solar Orbiter, RAM and others. EUV multilayers designed for relatively broad spectral response have also been deposited onto normal-incidence gratings in order to construct high-resolution spectrographs. The first satellite mission to utilize this approach will be the Solar-B/EIS instrument, currently under development and planned for launch in 2006.

Future solar missions utilizing normal-incidence multilayer optics for high-resolution imaging and/or spectroscopy will benefit greatly from possible improvements in multilayer performance, specifically higher reflectance, better spectral selectivity, and greater stability to heat, radiation and energetic particles. Additionally the development of new multilayers operating at longer EUV wavelengths, and at shorter EUV and soft X-ray wavelengths will make possible observations in otherwise-inaccessible solar emission lines, thereby providing better diagnostic tools for understanding the physics of the Sun.

In this paper we outline ongoing research and development of EUV and soft X-ray multilayers for solar physics. In ß2 we describe the performance of EUV multilayers containing silicon, operating at wavelengths longer than the Si L-edge at 12.4 nm, including recent results on new multilayers achieving higher reflectance, better spectral selectivity, and greater thermal stability. We also describe the recent development of the multilayer coatings used in the Solar-B/EIS instrument. We discuss prospects for new multilayer systems operating at longer EUV wavelengths in ß3, as well as EUV multilayers that work at wavelengths shorter than the Si L-edge in ß4. Finally in ß5 we describe recent progress in the development of ultra-short-period multilayers that work in the soft X-ray range at wavelengths shorter than $\lambda \sim 4$ nm. We summarize our results in ß6.

2. Si-BASED EUV MULTILAYERS

The low absorption of silicon at wavelengths longer than the Si L-absorption edge near $\lambda \sim 12.4$ nm has made this material an attractive and particularly successful constituent in a variety of EUV multilayer structures. The Si/Mo

Optics for EUV, X-Ray, and Gamma-Ray Astronomy, edited by Oberto Citterio, Stephen L. O'Dell, Proceedings of SPIE Vol. 5168 (SPIE, Bellingham, WA 2004)
0277-786X/04/$15 · doi: 10.1117/12.506175

multilayer system in particular is perhaps the most well-known and best-studied,[1,2,3] owing largely to its important application in photo-lithography as well as in solar physics. The normal-incidence reflectance attainable with Si/Mo approaches 70% just below the Si L-edge (where EUV lithographic steppers operate), though the reflectance falls steadily with increasing wavelength. The SOHO/EIT telescope[4] utilized Si/Mo multilayers, while the TRACE instrument[5] used a similar multilayer system comprising Si/Mo_2C bilayers, which gives better thermal stability, and a slightly narrower spectral response at the EUV wavelengths of interest for that mission (i.e., λ~17 ñ 29 nm).

Si/Mo multilayers will be used for the Solar-B/EIS instrument[6] as well, which employs a parabolic focusing mirror and a toroidal grating, both operating at normal incidence. In this instrument, each half of each optical element is coated with a broad-band multilayer; one channel is tuned to operate from $\lambda \sim$ 18 ñ 21 nm, the other tuned for $\lambda \sim$ 25 ñ 29 nm. These two wavelength bands include a number of bright lines from Fe X through Fe XXIV, as well as lines of He II, O V, Si VII, Si X, and Ca XVII. The spectrometer is designed to provide spectral resolution of order $\lambda/\Delta\lambda$~10,000, sufficient to determine Doppler velocities to an accuracy of ~3 km/s from spectral line shifts and non-thermal motions as small as 20 km/s from line widths. In order to maximize the scientific return from this instrument, the response of the multilayers must be optimized for both high reflectance and broad spectral response.

Multilayer coatings for the EIS optics were deposited by DC magnetron sputtering in argon, using a deposition system that has been described previously.[7] Preliminary EUV reflectance measurements of prototype coatings and flight optics were made using a laser-plasma-based reflectometer, also described previously,[7] while precision EUV calibration of the coated flight optics was performed using synchrotron radiation at NRL beamline X24C at the National Synchrotron Light Source. Further details regarding this work will be described elsewhere;[8,9] we present here a summary of some of our results.

The normal-incidence reflectance of prototype multilayer coatings for EIS are shown in Fig. 1. These coatings contain N=20 bilayers, with periods of order 10.4 and 14.4 nm for the short- and long-band channels, respectively. The fractional Si-layer-thicknesses for the films shown in Fig. 1a range from Γ=0.62 to 0.68, while those in Fig. 1b range from Γ=0.66 to 0.73; these results illustrate how the spectral response of the coatings can be fine-tuned by precisely varying the individual Si and Mo layer thicknesses. The measured multilayer curves shown in Fig. 1 were used to model the full EIS instrument response function, and based on these results, in consideration of the anticipated solar emission, the EIS optics were coated finally with Si/Mo films having d=10.42 nm, Γ=0.65 for the short-band channel, and d=14.4 nm, Γ=0.66 for the long-band channel.

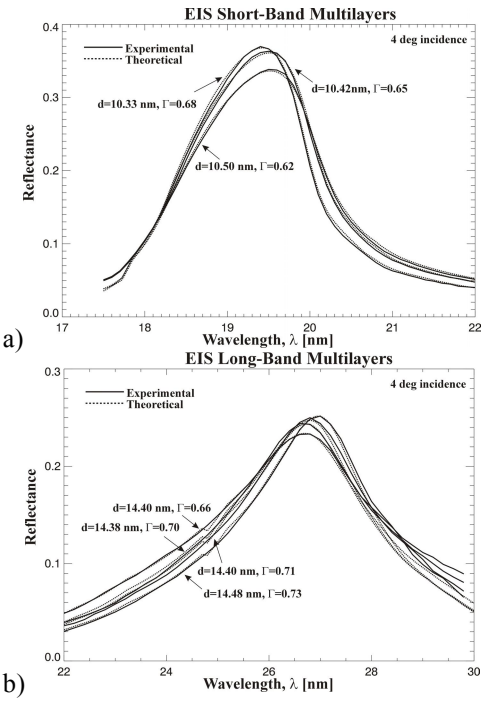

Figure 1. *Normal-incidence reflectance of prototype multilayers for the Solar-B/EIS instrument.*

The EIS flight optics were coated in fixtures that mask one half of the figured substrate during deposition, in order that separate coatings (i.e., tuned for short-band and long-band operation) could be deposited on each half of each substrate. Shadowing effects near the edges of the coating masks result in some small deviations in the coating thickness uniformity, particularly near the center of each substrate where, because of the substrate figure, the distance between the surface of the substrate and the edge of the mask is greatest. Nevertheless, the coating thickness uniformity that was achieved, shown for example in Fig. 2 for the case of the short-band coatings on the 6-inch-diameter focusing mirror, fully met the requirements for the EIS instrument. (Comparable uniformity was achieved on the toroidal grating as well.)

The wavelength range $\lambda \sim$ 25 ñ 35 nm is of particular interest for the development of future narrow-band solar imagers, as it includes diagnostically-important coronal and transition-region emission lines from Fe XV (28.4 nm), He II (30.4 nm), and Fe XVI (33.5 nm). At these wavelengths, however, the performance that can be achieved with Si/Mo is less than optimal: in particular, the peak reflectance of Si/Mo is low, and the spectral band-pass is wide enough to include significant spectral contamination from adjacent wavelengths due to emission from ions formed at other plasma temperatures. This is of particular concern especially in the vicinity of the

bright He II line at 30.4 nm. Future solar imaging missions therefore will benefit greatly from new multilayers having a more narrow spectral response in order to reduce such spectral contamination.

Si-based EUV multilayers other than Si/Mo that have been investigated previously include Si/Mo_2C, Si/B_4C and Si/C.[10,11] We have recently compared experimentally the performance of all of these coatings, as well as a new multilayer system comprising Si/SiC bilayers,[8] and we present some of our results here. Shown in Table 1 are the results obtained for an array of Si/Mo, Si/Mo_2C, Si/B_4C, Si/C and Si/SiC multilayers, all containing N=30 bilayers, with periods ranging from d~14.7 ñ 18.8 nm, designed for use near normal incidence at wavelengths in the range λ~28 ñ 34 nm. In order to achieve relatively narrow spectral response, we adjusted the factional Si-layer thicknesses $\Gamma=d_{Si}/d$ for each multilayer system, based on calculations using available optical constants. Narrow spectral response in the case of the Si/Mo and Si/Mo_2C multilayers requires relatively thin metal layers (~2 nm) for both of these systems, so the requisite Γ values are large: the actual values determined from X-ray reflectometry (XRR) using Cu Kα radiation (λ=0.154 nm) are Γ=0.86 for Si/Mo and Γ=0.89 for Si/Mo_2C. In contrast, because of their lower absorption at EUV wavelengths, multilayers containing B_4C, C, or SiC that achieve optimal narrow-band spectral response require thinner Si layers and thus smaller Γ values, in the range Γ=0.6 ñ 0.69 (i.e., comparable to the Γ values used in Si/Mo multilayers designed for high reflectance at shorter wavelengths, e.g., λ=13.4 nm, as in EUV lithography.)

For each of the five multilayer systems considered, we prepared films intended to be tuned to the emission lines of Fe XV (28.4 nm), He II (30.4 nm), and Fe XVI (33.5 nm). The EUV reflectance results made using synchrotron radiation at NSLS, also listed in Table 1, revealed that the peak wavelengths in all cases were systematically shorter than the target wavelengths, typically by δλ~1 nm; schedule and resource limitations precluded the possibility of preparing new samples with corrected, slightly larger periods. However, the measured peak wavelengths are close enough to the target wavelengths, arguably, to warrant relative comparisons between the different multilayers, and to justify the conclusions we draw below regarding the utility of these coatings for future solar instruments.

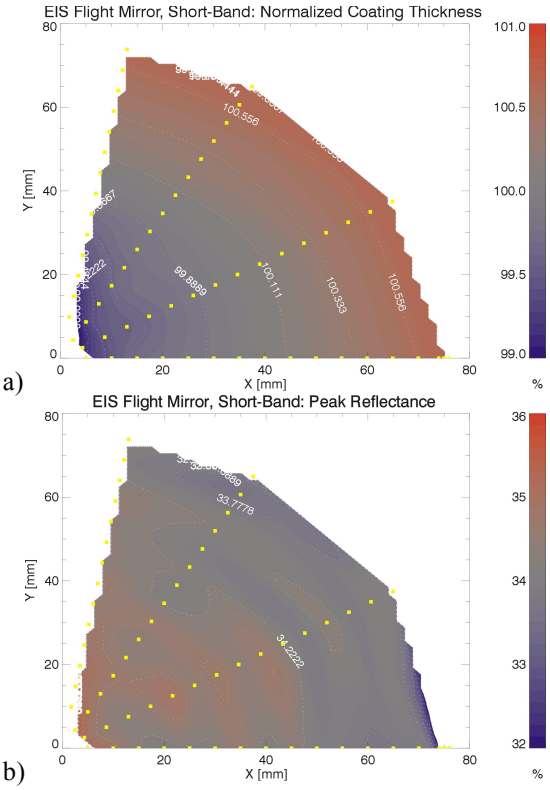

Figure 2. *Coating thickness (a) and peak reflectance (b) uniformity maps for the short-band multilayer coatings deposited on the EIS 6-inch primary mirror. Measurements were made over one quadrant of the mirror at the positions of the yellow squares; smooth contours were drawn using bilinear spline interpolation between the measured points.*

Materials	N	d [nm]	Γ_{Si}	R_{max}	λ_{max} [nm]	FWHM [nm]	Rejection
Si/Mo	30	14.88	0.86	22.4%	27.9	1.610	6.6X to 30.4 nm
		16.00	0.86	19.7%	29.9	1.452	4.3X to 28.4 nm
		17.98	0.87	15.5%	32.9	1.525	5.2X to 30.4 nm
Si/Mo $_2$ C	30	14.73	0.89	19.0%	27.8	1.390	9.6X to 30.4 nm
		15.95	0.89	15.8%	29.8	1.398	4.9X to 28.4 nm
		17.73	0.89	13.1%	32.7	1.447	6.2X to 30.4 nm
Si/B $_4$ C	30	15.20	0.69	35.3%	28.1	1.584	7.0X to 30.4 nm
		16.45	0.69	29.1%	29.8	1.970	7.7X to 28.4 nm
		18.75	0.69	26.5%	32.9	2.060	10.3X to 30.4 nm
Si/C	30	14.70	0.65	19.0%	27.5	1.600	4.7X to 30.4 nm
		15.80	0.65	17.8%	29.4	1.980	5.3X to 28.4 nm
		17.80	0.65	16.9%	32.3	2.570	7.1X to 30.4 nm
Si/SiC	30	15.05	0.60	18.5%	27.9	1.272	13.1X to 30.4 nm
		16.43	0.60	17.2%	29.8	1.470	14.0X to 28.4 nm
		18.25	0.60	16.7%	32.8	1.713	26.8X to 30.4 nm

Table 1. *Experimental results obtained with Si/Mo, Si/Mo_2C, Si/B_4C, Si/C, and Si/SiC multilayers.*

To facilitate such relative performance comparisons (particularly the spectral selectivities derived below), we show in Fig. 3 the measured normal-incidence reflectance curves of the samples listed in Table 1, where we have adjusted slightly the wavelength scale for each sample independently in these plots so that the peak wavelengths overlap. The highest peak reflectance by far at all wavelengths is obtained with the Si/B_4C multilayer system, which achieves normal incidence reflectance ranging from 35.1% at λ=28.1 nm to

26.5% at λ=32.9 nm. These reflectance values are considerably higher than those achieved using the traditional Si/Mo and Si/Mo_2C multilayers used in previous solar instruments (e.g.., Si/Mo ranges from 22.4% to 15.5% over the same approximate wavelength range, while the reflectance of Si/Mo_2C is comparable), indicating that significant improvements in efficiency can be realized in future instruments utilizing this coating. For example, the efficiency of a two-reflection Cassegrain-type telescope tuned near 30 nm would more than double if it utilized Si/B_4C rather than Si/Mo coatings. The peak reflectance obtained with Si/C ranges from 19% to 16.9% over the range 27.5 ñ 32.3 nm; these values are smaller than the values of 20% at 28.3 nm, and 25% at 30.4 nm for comparable Si/C films reported in reference [11], and the reason for this discrepancy is not known. The peak reflectances measured for Si/SiC multilayers are similar to those of Si/C, ranging from 18.5% to 16.7% over the same approximate range of wavelengths, though the spectral response of Si/SiC is much more narrow.

In addition to its higher reflectance, Si/B_4C can provide considerably greater spectral selectivity relative to Si/Mo, Si/Mo_2C, and Si/C. Although the measured full-width-half-maximum (FWHM) response of Si/B_4C increases at longer wavelengths, ranging from FWHM=1.58 nm to 2.40 nm over the same wavelength range, whereas the FWHM of Si/Mo, for example, is approximately constant at ~1.5 nm over this range, the effective spectral selectivity of Si/B_4C nevertheless exceeds Si/Mo (as well as Si/Mo_2C and Si/C) at all wavelengths. We can characterize quantitatively the spectral selectivity of multilayer coatings in a way that is particularly useful with regard to the design of solar imaging instruments, by computing the effective rejection factor to adjacent wavelengths. We define this rejection factor as the peak reflectance at the target wavelength divided by the peak reflectance at the wavelength of the nearest bright solar emission line. We list rejection factors for each multilayer in the last column of Table 1; the rejection factors for coatings tuned to the Fe XV and Fe XVI lines refer to rejection of He II 30.4 nm radiation, while the rejection factor for He II multilayers refers to rejection of Fe XV emission at 28.4 nm. As can be seen from the table, the rejection factors for Si/B_4C exceed those of Si/Mo, Si/Mo_2C and Si/C in all cases; however the highest spectral selectivity by far is obtained with Si/SiC multilayers: the rejection factor for Si/SiC ranges from 13.1X for a coating tuned to 28.4 nm, to 26.8X for a coating tuned to 33.5 nm. In comparison, the rejection factors for Si/B_4C range from 7X to 10.3X over this same range, while the rejection factors for the other three multilayer systems are lower still. (Note that the rejection factors for a two-reflection telescope scale as the square of the numbers listed in Table 1.) Considering the relative intensity of the bright He II 30.4 nm line to the weaker Fe XVI 33.5 nm line, the greater spectral selectivity obtained with Si/SiC at the Fe XV and Fe XVI lines in particular, albeit with lower peak reflectance, may make this the preferred coating in many cases for these wavelengths. For example, assuming that the He II line is six times brighter than the Fe XVI line,[12] a two-reflection

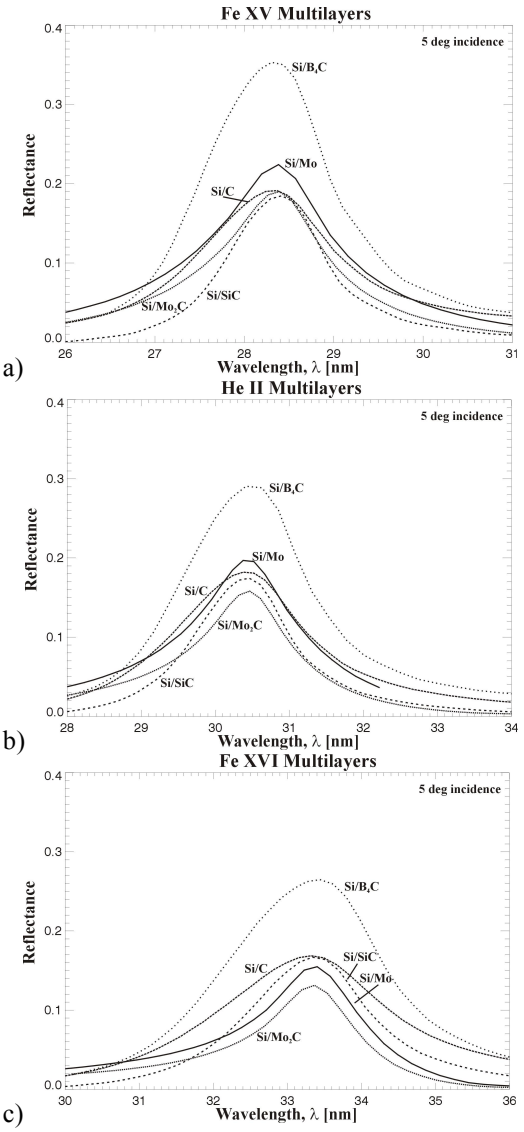

Figure 3. *Measured EUV reflectance of Si/Mo, Si/Mo_2C, Si/B_4C, Si/C and Si/SiC multilayers tuned near the solar Fe XV line at 28.4 nm (a), the He II line at 30.4 nm (b), and the Fe XVI line at 33.5 nm (c). The structural parameters for each multilayer is listed in Table 1. The reflectance was measured at 5 deg incidence using synchrotron radiation at NSLS. The wavelength scale was adjusted slightly for each multilayer in these plots to compensate for small variations in multilayer period between samples, in order to facilitate relative performance comparisons.*

telescope tuned to the Fe XVI line would result in only ~0.8% spectral contamination using Si/SiC coatings, but ~5.7% contamination using Si/B_4C; the spectral contamination obtained using any of the other coatings would be even greater, e.g., 22% contamination with Si/Mo. (The spectral selectivity of coatings tuned to the He II line is a far less important consideration, given the relative brightness of this line.)

The suitability of EUV multilayer coatings for use in space missions for solar physics depends not just on their EUV performance, but also on their long-term stability to heat, radiation and energetic particles. These characteristics will become especially important with future mission such as Solar Orbiter, whose planned orbit will take the spacecraft to within 45 solar radii (0.2 AU), thereby presenting an extreme environment to the constituent instruments.[13] We have assessed the thermal stability of the five multilayer systems just described by measuring the X-ray and EUV reflectance of each of these films before and after thermal anneals at 100 C, 200 C, and 300 C. The films were placed on a hot-plate heated to the specified temperatures, and held for one hour (in air) in order to promote any possible microstructural changes that might occur.

Shown in Fig. 4 are the measured EUV reflectance* curves for the films tuned near the Fe XV line described above. With the notable exception of the Si/SiC film, all of the multilayers show some degradation in peak EUV reflectance; corresponding changes were observed in the XRR data (not shown here) suggesting microstructural changes. The Si/Mo and Si/C films also show significant shifts in the peak wavelength, corresponding to a decrease or an increase, respectively, in the multilayer period. The decrease in peak reflectance observed in the Si/Mo_2C film is slight. In contrast to these four multilayer systems, the peak EUV reflectance of the Si/SiC film actually increases slightly after thermal annealing.

A number of annealing-induced microstructural changes can explain the results shown in Fig. 4, including interfacial reaction, interfacial diffusion, compound formation, or any combination of these mechanisms. Without more detailed studies, we cannot untangle these effects and identify with certainty the precise explanation in each case. Nevertheless, we can conclude from the results presented here that all of these multilayers are reasonably stable when held to temperatures below 100 C, which will be quite likely the maximum temperature experienced during any future solar mission as currently conceived. The stability to radiation and energetic particles remains to be explored, however.

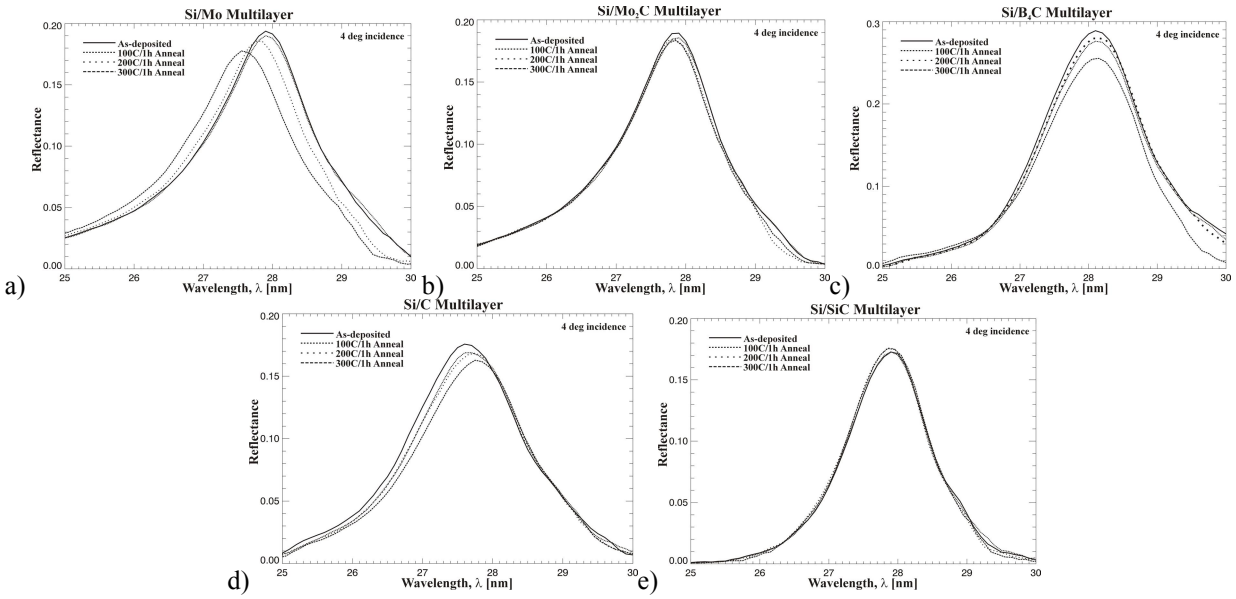

Figure 4. *Measured normal-incidence EUV reflectance of Si/Mo (a), Si/Mo_2C (b), Si/B_4C (c), Si/C (d), and Si/SiC (e) multilayers, comparing the response for as-deposited films vs. films annealed for 1 hour at 100 C, 200 C, and 300 C as indicated. The reflectance measurements in this case were made at 4 deg incidence using a laser-plasma-based reflectometer.*

* These EUV reflectance data were obtained using the laser-plasma-based reflectometer mentioned above; in this case no adjustments to the wavelength scales were made.

3. LONG-WAVELENGTH EUV MULTILAYERS

At EUV wavelength longer than ~40 nm, a region that spans several important solar lines including Ne VII (46.5 nm), O V (63.9 nm) and O III (83.5 nm), the ability to develop efficient multilayer coatings has been limited thus far by the lack of suitable materials having low absorption; high absorption prevents incidence EUV radiation from penetrating deeply into the multilayer and reflecting from many interfaces, thereby undermining the effectiveness of these thin-film interference devices.

The most promising results to date have involved multilayers comprising Sc layers,[14] a material found to have relatively low absorption at wavelengths longer than ~35 nm as a result of its 3d open shell. In particular, Sc/Si multilayers, utilizing thin W barrier layers to mitigate interfacial reaction, have been measured to give peak reflectance values of ~20 ñ 30 % near normal incidence in the 35 ñ 45 nm wavelength range; new results demonstrating a peak reflectance of 56% in this wavelength range have been reported recently as well.[15]

A number of other materials may show similarly low absorption, and might prove useful in the construction of either broad-band or narrow-band multilayers. For example, shown in Fig. 5 are theoretical reflectance curves for a variety of La multilayers, tuned near the O V line at 63.9 nm. These calculations were made using optical constants determined from the CXRO atomic scattering factors,[16] which suggest low absorption near the La 5d open shell. For narrow-band imaging at this wavelength, it will be necessary to minimize the reflectance near ~61 nm, in order to suppress spectral contamination from other relatively bright solar lines; the results shown in Fig. 5 are encouraging in this regard. Experiments are now underway to determine how well these and other candidate multilayers actually perform.

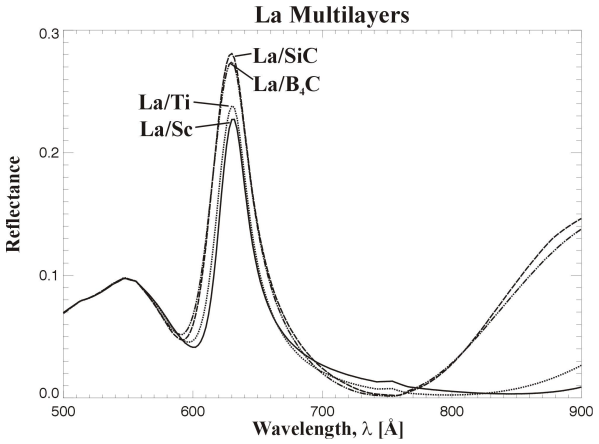

Figure 5. *Theoretical reflectance of La multilayers tuned near the O V line at 63.5 nm.*

4. SHORT-WAVELENGTH EUV MULTILAYERS

At wavelengths shorter than the Si L-edge, a number of efficient new multilayer systems have recently emerged. In particular, the Mo/Y multilayer system[17,18] has been shown to have good reflectance (R~34 ñ 38%) near the diagnostically important Fe XVIII line at 9.39 nm. We have recently compared prototype Fe XVIII multilayers comprising Mo/Y, Ru/B_4C and Ru/Y multilayers, and the results, obtained using synchrotron radiation at Beamline 6.3.2 at the ALS, are shown in Fig. 6. (We have once again shifted the wavelength scale slightly for these reflectance curves in order to facilitate relative performance comparisons.) In this study, Mo/Y indeed provides the highest reflectance: we find R=34% for this sample, compared with 28.3% for the previously-investigated Ru/B_4C system,[19] and a disappointing 21.4% for the new Ru/Y system. (The optical constants of Ru and Y suggest that the reflectance of this system could be highest of all, provided that smooth, sharp interfaces can be achieved, which is apparently not the case.) Another new multilayer system showing high reflectance below 10 nm is the La/B_4C multilayer system,[20] for which peak normal incidence reflectance of 39% has been achieved[21] near the Si VII line at 7.3 nm.

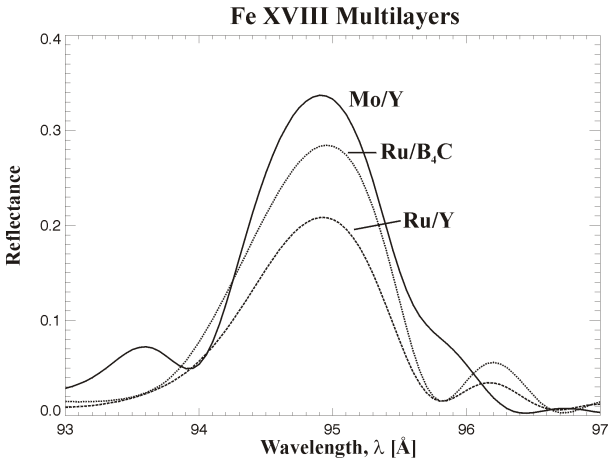

Figure 6. *Comparison of experimental reflectance of Mo/Y, Ru/B4C and Ru/Y multilayers tuned near the Fe XVIII line at 9.39 nm. The measurements were made using synchrotron radiation at Beamline 6.3.2, Advanced Light Source. The wavelength scale was adjusted slightly for each multilayer to compensate for small variations in multilayer period between samples.*

5. ULTRA-SHORT-PERIOD SOFT X-RAY MULTILAYERS

We discuss here the possible utility and availability of ultra-short-period multilayer coatings operating near normal incidence in the soft X-ray region, specifically in the vicinity of the important C VI (3,4 nm), O VII (2.2 nm) and O VIII (1.9 nm) resonance lines, and the Fe XVII 3sñ2p (1.7 nm) and 3dñ2p (1.5 nm) transition line complexes. These soft X-ray lines represent the primary emission at active region temperatures (Fig. 7). The Fe XVII lines especially dominate the coronal X-ray spectrum from 3ñ5x10^6 K (Fig. 8), corresponding to the bulk of the differential emission measure (DEM) in active regions,[22] yet there are no observable lines from this ion in the EUV where multilayer imagers now operate. The oxygen lines are dominant in the 2ñ 3x10^6 K region, which makes them ideal for studying coronal mass ejections (CMEs) and the features interconnecting active regions, as well as those structures likely to be involved in large-scale reconnections related to CMEs.

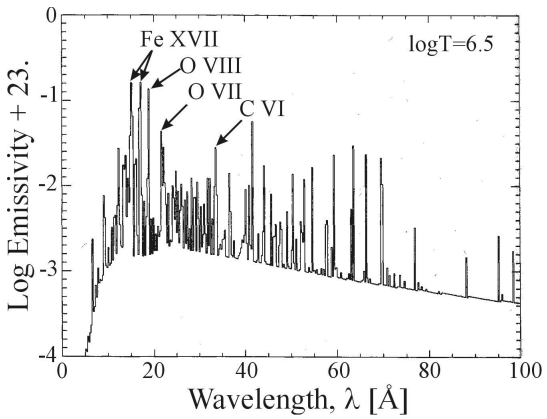

Figure 7. *Solar spectral emissivity at logT=6.5. The soft X-ray region below 3.5 nm is dominated by C VI, O VII, O VIII and Fe XVII.*

A soft X-ray imager tuned to the C VI line (~1.3x10^6 K) would facilitate better observations of the complicated transition region topology, particularly the connections between the high pressure coronal loops and the top of the transition region, which are difficult to observe using, e.g., Fe X emission (λ~17.4 nm) because of obscuration by spicules that are strongly-absorbing in the EUV. But this portion of the X-ray spectrum has only been accessible until now using grazing incidence X-ray optics, which have intrinsically broad spectral response. The features observed in broad-band soft X-ray images of the solar corona (as from Yohkoh-SXT, for example) are generally not as sharply defined as in narrow-band EUV images of the same location (e.g., as from SOHO/EIT or TRACE, although the latter instrument also has intrinsically higher angular resolution relative to Yohkoh-SXT.) In addition to the higher angular resolution attainable with normal-incidence telescope mirrors, the difference in spectral response between grazing vs. normal-incidence telescopes also leads to sharper images, since the broad spectral response of grazing incidence instruments produces images of emission from plasma having a relatively wide distribution of temperatures, effectively blurring the image (since each plasma component has its own spatial distribution.)

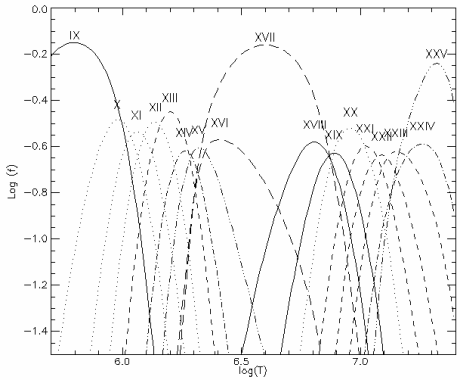

Figure 8. *Ionization fraction of Fe as a function of temperature. Fe XVII dominates the 3ñ5x10^6 K range.*

By extending the performance of narrow-band, normal-incidence multilayer instruments to the soft X-ray, where the expected multilayer spectral response is even more narrow than in the EUV, in fact, we will be able to isolate individual spectral lines, which will allow us to obtain high-resolution, quasi-iso-thermal images that more clearly delineate the topology and dynamics of active regions, the onset and early development of CMEs, and the transition region foot points of high pressure coronal loops. Imaging the emission from just a single ion will make the interpretation of the observations easier and will allow for detailed comparison with state-of-the-art coronal simulations. Furthermore, it may be possible to use these new coatings to observe density-sensitive soft X-ray line pairs in order to provide important physical constraints on active regions and flares.

In the soft X-ray region, the absorption of candidate multilayer materials is significantly lower than in the EUV, suggesting, in principle, that highly efficient multilayers can be constructed containing hundreds of periods. In practice, however, interface imperfections ñ roughness and diffuseness ñ have thus far limited greatly the achievable peak reflectance. The best results so far have been obtained with two new multilayer systems, one containing Cr/Sc bilayers,[23,24] the other containing W/B_4C bilayers[25].

Cr/Sc multilayers designed for use above the Sc L-edge (λ ~ 3.1 nm) can now be fabricated with peak reflectance values of order 5.5% over a spectral bandpass of Δλ~0.012 nm near the C VI line at λ=3.37 nm. To

illustrate, shown in Fig. 9 are the reflectance curves measured near normal incidence (2.5°) as a function of wavelength, for three prototype Cr/Sc films, each containing N=300 bilayers, with periods d=1.87 nm, 1.73 nm, and 1.60 nm as indicated. (The coating used in an actual solar telescope of course would be tuned precisely to the C VI line.) The reflectance increases towards shorter wavelengths because absorption in the Sc layers decreases close to the L-edge. The interface widths deduced from fits to the measured reflectance curves are of order σ~0.4 nm, and, following the work of reference [24], were obtained by using a substrate bias of ñ28 V during deposition, used to optimize the kinetic energy of argon ions striking the surface of the growing film in order to minimize interfacial roughness.

At shorter wavelengths, even smaller interface widths have been obtained with W/B_4C multilayers having periods as small as d=0.8 nm. Shown in Fig. 10 are the normal incidence reflectance curves measured for a series of W/B_4C films, also having 300 bilayers, with periods in the range d=0.8 ñ 1.2 nm. The interface widths determined from the fits to these measurements are σ~0.29 nm. As can be seen in the figure, normal incidence reflectance was measured at wavelengths as short as 1.6 nm.

Even better performance could be achieved at these short wavelengths, in principle, using materials having lower absorption, and using deposition techniques that give rise to smaller interface widths. In particular, the electronic structure of the 3d transition elements Sc through Ni is such that all these elements exhibit prominent L-edge absorption features in the soft X-ray region from λ=1.5 ñ 3.1 nm. The low absorption of these materials on the long-wavelength side of these L-edge features, as illustrated in Fig. 11, gives rise to a number of highly promising material combinations for potential use

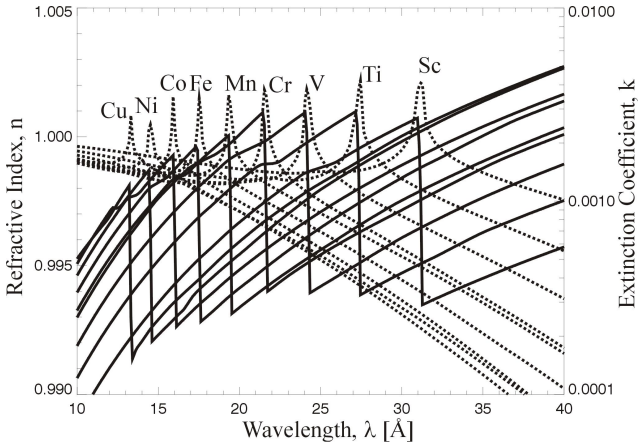

Figure 10. *Optical constants of some 3d transition elements having strong absorption edges in the soft X-ray.*

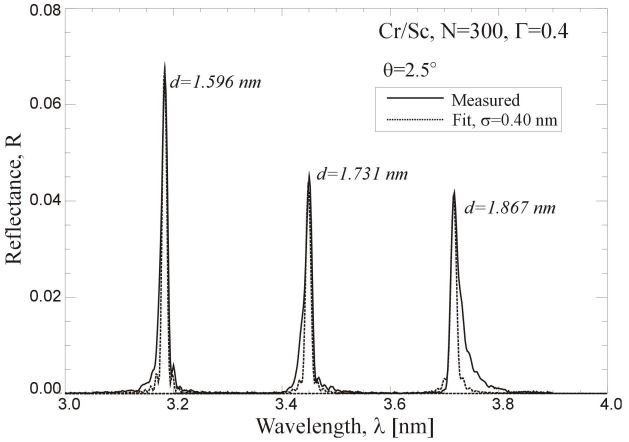

Figure 9. *Normal-incidence reflectance of periodic Cr/Sc multilayers, measured at Beamline 6.3.2 at the ALS.*

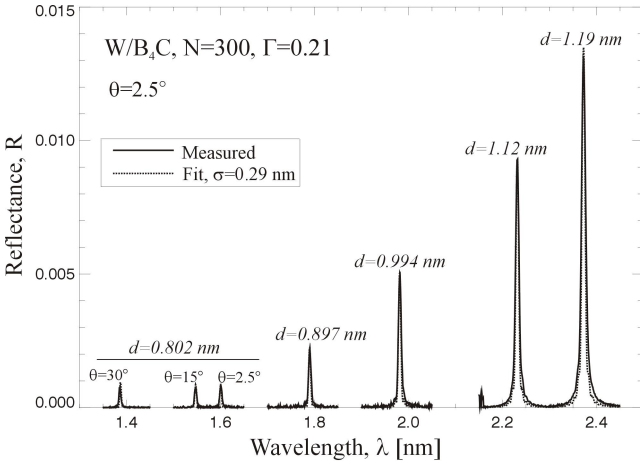

Figure 10. *Normal-incidence reflectance of periodic W/B_4C multilayers, measured (using s-polarized light) at Beamline 6.3.2 at the ALS.*

in multilayers designed for these short wavelengths. We hope to investigate many such candidate material combinations in the future.

The peak reflectance of ultra-short-period soft X-ray multilayers achieved thus far is relatively small, but is nevertheless close to what will be required to construct a practical high resolution soft X-ray imager. We have estimated fluxes at 1 AU for the coronal soft X-ray lines mentioned above, as a function of temperature, integrated over a spectral bandpass of $\Delta\lambda=0.1$ ≈. These fluxes were computed using the SAO Astrophysical Plasma Emission Code,[26] assuming coronal abundances and a volume emission measure of $1x10^{44}$ cm^{-3}, characteristic of a bright active region at ~$3x10^6$ K. We have then used the peak flux values to estimate the required multilayer

performance necessary to construct a practical high-resolution telescope: we assume a 20-cm-diameter primary mirror, and have set the requisite signal-to-noise ratio to 100 photons/pixel. Our estimates indicates that, for example, the Fe XVII line at 1.7 nm can be imaged with 1 arcsec pixels and 1 second cadence in a Cassegrain telescope even if just 1% multilayer reflectance is achieved; higher reflectance will allow for even greater resolution and cadence. With continued multilayer research this level of performance is perhaps not that far from being realized.

6. SUMMARY

We have attempted to provide an overview of currently available EUV multilayer coatings that can be used in solar physics instrumentation comprising normal-incidence optics; we present in Fig. 12 a plot summarizing some of the recent results described here. We have also outlined some prospects for future research involving new multilayer material combinations which could lead to improved performance, and wider spectral coverage, specifically at the long- and short-wavelength extremes.

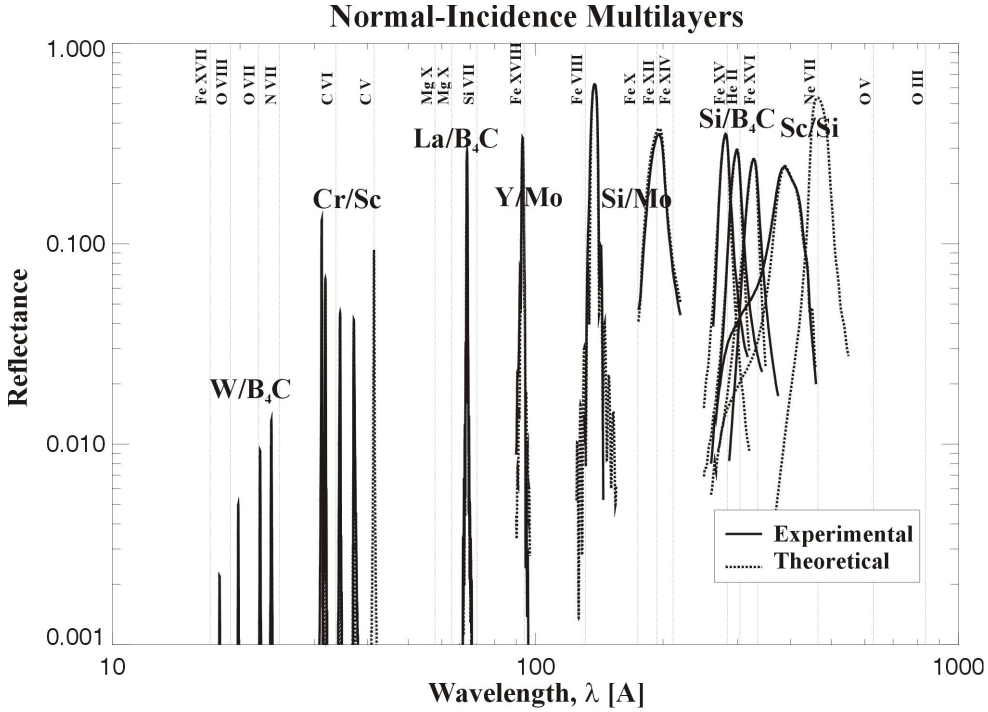

Figure 12. *Some of the recent multilayer results discussed in the paper are summarized here.*

The excellent EUV performance achieved using Si/Mo multilayers has led to a number of successful missions, including SOHO/EIT and TRACE; broad-band Si/Mo multilayers will be used for the Solar-B/EIS instrument as well. Looking ahead, new Si-based multilayers may offer improved performance relative to Si/Mo for future solar missions: in particular, we have shown how Si/B_4C multilayers offer significantly higher reflectance, and greater spectral selectivity in the range $\lambda \sim 25$ ñ 35 nm, while the new Si/SiC multilayer system offers the greatest thermal stability, and the highest spectral selectivity in the vicinity of the bright He II line at 30.4 nm which can easily contaminate high-resolution images at adjacent wavelengths.

Complementary to recently developed Si/W/Sc multilayers, new long-wavelength multilayers containing La or other low-absorption materials may lead to new capabilities near the Ne VII (46.5 nm), O V (62.9 nm), and O III (83.5 nm) EUV lines. At shorter wavelengths, efficient Mo/Y and La/B_4C multilayers can now be used near the Fe XVIII (9.4 nm) and Si VII (7.3 nm) lines, respectively, while emerging ultra-short-period multilayers, such as Cr/Sc, W/B_4C and others may lead eventually to the development of narrow-band imagers operating in the soft X-ray, specifically near the C VI (3.37 nm), O VII (2.2 nm), O VIII (1.9 nm), and Fe XVII (1.7 and 1.5 nm) lines that dominate the coronal X-ray spectrum from 3ñ5x10^6 K.

ACKNOWLEDGEMENTS

The authors would like to acknowledge a number of individuals and groups for their important contributions to this research: A. Aquila (ALS) for reflectance measurements; C. Brown, K. Dere, G. Doschek, C. Korendyke, J. Mariska, S. Myers, and the entire NRL Solar-B/EIS team for their financial support as well as important contributions regarding the EIS multilayer requirements; R. Howard, D. Moses and J. Newmark for their support in the development of long-wavelength EUV multilayers; and L. Harra and J. L. Culhane (MSSL) for important discussions regarding the stability of EUV multilayers for Solar Orbiter.

This research was sponsored in part by a grant from NASA.

REFERENCES

[1]D. G. Stearns, M. B. Stearns, Y. Cheng, J. H. Stith, N. M. Ceglio, ëThermally induced structural modification of Mo-Si multilayersí, *J. App. Phys*., 67, 2415, (1990)

[2] J. M. Slaughter, A. Shapiro, P. A. Kearney, and C. M. Falco, ëGrowth of molybdenum on silicon: structure and interface formationí, *Phys. Rev. B*, 44, 3854 (1991)

[3] D. L. Windt, R. Hull, and W. K. Waskiewicz, `Interface imperfections in metal/Si multilayersí, *J. Appl. Phys.*, 71, 2675-2678 (1992)

[4]J. P. DelaboudiniËre, G. E. Artzner, J. Brunaud, A. H. Gabriel, J. F. Hochdez, F. Millier, X. Y. Song, B. Au, K. P. Dere, R. A. Howard, R. Kreplin, D. J. Michels, J. D. Moses, J. M. Defise, C. Jamar, P. Rochus, J. P. Chauvineau, J. P. Marioge, R. C. Catura, J. R. Lemen, L. Shing, R. A. Stern, J. B. Gurman, W. M. Neupert, A. Maucherat, F. Clette, P. Cugnon and E. L. Van Dessel , ëEIT: Extreme-ultraviolet imaging telescope for the SOHO missioní, *Solar Physics* 162, 291 ñ 312 (1995)

[5]B. N. Handy, L. W. Acton, C. C. Kankelborg, C. J. Wolfson, D. J. Akin, M. E. Bruner, R. Caravalho, R. C. Catura, R. Chevalier, D. W. Duncan, C. G. Edwards, C. N. Feinstein, S. L. Freeland, F. M. Friedlander, C. H. Hoffmann, N. E. Hurlburt, B. K. Jurcevich, N. L. Katz, G. A. Kelly, J. R. Lemen, M. Levay, R. W. Lindgren, D. P. Mathur, S. B. Meyer, S. J. Morrison, M. D. Morrison, R. W. Nightingale, T. P. Pope, R. A. Rehse, C. J. Schrijver, R. A. Shine, L. Shing, T. D. Tarbell, A. M. Title, D. D. Torgerson, L. Golub, J. A. Bookbinder, D. Caldwell, P. N. Cheimets, W. N. Davis, E. E. DeLuca, R. A. McMullen, D. Amato, R. Fisher, H. Maldonado, and C. Parkinson, ëThe Transition Region and Coronal Explorer,í *Solar Physics,* 187, 229 ñ 260 (1999)

[6] J. Seely, ëMultilayer grating for the Extreme Ultraviolet Spectrometer (EIS)í, SPIE, 4138, 174 ñ 181 (2002)

[7] D. L. Windt and W. K. Waskiewicz, ëMultilayer facilities required for extreme-ultraviolet lithographyí, *J. Vac. Sci. Technol. B*, 12, 3826 ñ 3832 (1994)

[8] D. L. Windt, S. Donguy, J. Seely, B. Kjornrattanawanich, ëExperimental comparison of extreme ultraviolet multilayer coatings for solar physicsí, submitted to *App. Opt*.

[9] J. Seely, *et al*., these proceedings.

[10] J. M. Slaughter, B. S. Medower, R. N. Watts, C. Tarrio, T. B. Lucatorto, and C. M. Falco, ëSi/B_4C narrow-bandpass mirrors for the Extreme Ultravioletí, *Opt. Lett*., 19, 1786 (1994)

[11] M. Grigonis and E. J. Knystautas, ëC/Si multilayer mirrors for the 25-30 nm wavelength regioní, *App. Op*. 36, 2839 (1997)

[12]R. J. Thomas and W. M. Neupert, ëExtreme ultraviolet spectrum of a solar active region from SERTSí, *Ap. J. S*., 91, 461 ñ 482 (1994)

[13] Solar Orbiter Assessment Study Report, July 2000, and Pre-Assessment Study Report, October 1999:<http://zeus.nascom.nasa.gov/~bfleck/Orbiter/Documents/pre_assess_rep.pdf>

[14] J. F. Seely, Yu. A. Uspenskii, Yu. P. Pershin, V. V. Kondratenko, and A. V. Vinogradov, "Skylab 3600 groove/mm replica grating with a scandium-silicon multilayer coating and high normal-incidence efficiency at 38 nm wavelength," *App. Opt*. 41, 1846 (2002).

[15] F. Schaefers, S. Yulin, T. Feigl, and N. Kaiser, *Eight International Conference on Synchrotron Radiation Instrumentation*, San Francisco, CA, 2003

[16] B. L. Henke, E. M. Gullikson, and J. C. Davis, ëX-ray interactions: photabsorption, scattering, transmission, and reflection at E=50-30,000 eV, Z=1-92', *At. Data Nuclear Data Tables*, 54, 181 (1993)

[17] B. Sae-Lao, S. Bajt, C. Montcalm, and J. F. Seely, ëPerformance of normal-incidence molybdenumñyttrium multilayer-coated diffraction grating at a wavelength of 9 nmí, *App. Op*., 41, 2394 ñ 2400 (2002)
[18] C. Montcalm, P. A. Kearney, J. M. Slaughter, B. T. Sullivan, M. Chaker, H. PÈpin, and C. M. Falco, ëSurvey of Ti-, B-, and Y-based soft x-rayñextreme ultraviolet multilayer mirrors for the 2- to 12-nm wavelength regioní, App. Op., 35, 5134 ñ 5147 (1996)
[19] D. G. Stearns, R. S. Rosen, and S. P. Vernon, ëNormal incidence X-ray mirror for 7 nmí, *Opt. Let*., 16, 1283 ñ 1285 (1991)
[20] P. Ricardo, R. G. Wiesmann, C. Nowak, C. Michaelsen, D. Bormann, ëImproved Analyzer Multilayers for Aluminium and Boron Detection with X-Ray Fluorescenceí, *App. Op*., 40, 2747-2754 (2001)
[21] Y. Platonov; reported on the CXRO Multilayer Survey website: <http://www-cxro.lbl.gov/multilayer/survey.html>
[22] ì The Solar Coronaî, L. Golub and J. Pasachoff, Cambridge Univ. Press, Cambridge, UK, 1997
[23] F. Schäfers, M. Mertin, D. Abramsohn, A. Gaupp, H.-Ch. Mertins, and N. N. Salashchenko, ëCr/Sc nanolayers for the water window: improved performanceí, *Nucl. Instr. Meth. A*, 467-468, 349 (2001)
[24] F. Eriksson, G. A. Johansson, H. M. Hertz, and J. Birch, ëEnhanced soft x-ray reflectivity of Cr/Sc multilayers by ion-assisted sputter depositioní, *Proc. SPIE*, 4506, 14 (2001)
[25] D. L. Windt, E. M. Gullikson, C. C. Walton, ëNormal-incidence reflectance of optimized W/B_4C multilayers in the range 1.4 nm < λ < 2.4 nmí, *Opt. Lett.,* 27, 2212-2214 (2002)
[26] APEC Version 1.1; <http://asc.harvard.edu/atomdb>